

**NASA  
Technical  
Memorandum**

NASA TM - 100315

DEVELOPMENT OF OPTICAL MODULATORS FOR  
MEASUREMENTS OF SOLAR MAGNETIC FIELDS

CENTER DIRECTOR'S DISCRETIONARY FUND FINAL REPORT

By E. A. West and J. E. Smith

Space Science Laboratory  
Science and Engineering Directorate

October 1987

(NASA-TM-100315) DEVELOPMENT OF OPTICAL  
MODULATORS FOR MEASUREMENTS OF SOLAR  
MAGNETIC FIELDS Final Report (NASA)

35 p  
CSCL 20F

N88-13016

Unclas  
G3/74 0106524



National Aeronautics and  
Space Administration

**George C. Marshall Space Flight Center**

## TABLE OF CONTENTS

	Page
<b>I. INTRODUCTION</b> .....	1
<b>II. DISCUSSION</b> .....	2
A. Data Acquisition System .....	4
B. LCD Modulator .....	5
1. Camera Shutter .....	7
2. Variable Waveplate .....	8
C. KD*P Modulator .....	9
1. Variable Waveplate .....	12
2. Camera Shutter .....	12
<b>III. CONCLUSIONS</b> .....	13
<b>REFERENCES</b> .....	14
<b>APPENDIX</b> .....	15

PRECEDING PAGE BLANK NOT FILMED

## LIST OF ILLUSTRATIONS

Figure	Title	Page
1.	Schematic diagram showing the location of optical modulators used in the Marshall Space Flight Center Vector Magnetograph .....	16
2.	Timing diagram showing the relationship between the polarimeter timing and the shutter timing required for LCD and KD*P modulators .....	17
3.	Diagram of the data acquisition system .....	18
4.	Diagram of the director orientation for an untwisted and twisted nematic liquid crystal in the presence of an electric field .....	19
5.	The orientation of the indices of refraction in a twisted nematic liquid crystal .....	20
6.	The spatial variation of the contrast ratio in a liquid crystal modulator .....	21
7.	Poincaré sphere the orientation and retardation of two LCD modulators aligned to reduce the retardation errors cause by boundary effects .....	22
8.	The time response of large LCD modulators .....	23
9.	Diagram showing the movement of the deuterium atom in the KD*P crystal with applied electric field .....	23
10.	Schematic of a KD*P modulator with the electrode and insulating coatings .....	24
11.	Diagram of the electrical equivalent and response of a KD*P crystal .....	25

**LIST OF ILLUSTRATIONS (Concluded)**

Figure	Title	Page
12.	Areas of high resistivity in the ITO coatings of a KD*P modulator .....	26
13.	Diagram indicating that resistivity and capacitance will vary spatially over the KD*P modulator .....	27

## LIST OF TABLES

Table	Title	Page
1.	Design Goals for Electronic Modulators to be Used in the MSFC Vector Magnetograph .....	3
2.	Requirements for an Electrooptical Modulator Used as a Polarization Analyzer in the MSFC Vector Magnetograph.....	3
3.	Requirements for an Electrooptical Modulator Used as a Camera Shutter in the MSFC Vector Magnetograph .....	3
4.	Thickness Required for Halfwave Retardation at $\lambda = 6328 \text{ \AA}$ for Various LCD Compounds .....	6
5.	Resistivity in KD*P Samples .....	11

## DEFINITION OF SYMBOLS

$\delta$	retardance
$\lambda$	wavelength of light
$n_e$	extraordinary index of refraction
$n_o$	ordinary index of refraction
$n_x$	index of refraction along the x axis
$n_y$	index of refraction along the y axis
$T$	thickness

## STANDARD ABBREVIATIONS

CCD	charge coupled device
ITO	indium tin oxide
LCD	liquid crystal device
KD*P	potassium dideuterium phosphate
RC	resistor - capacitor

## NONSTANDARD ABBREVIATIONS

EOC	electrooptical crystal
PEM	photoelastic modulator
PLZT	lanthanum-modified lead zircoate titanate
EM	electrooptic modulator

## UNUSUAL TERMS

A	used to describe the timing of the polarimeter and the polarization measurement obtained when a positive quarterwave retardation is applied to the polarization modulator
B	used to describe the timing of the polarimeter and the polarization measurement obtained when a negative quarterwave retardation is applied to the polarization modulator
F1	a type of failure seen in KD*P modulators where the retardation characteristics do not follow the applied voltage
F2	a type of failure seen in KD*P modulators where the retardation characteristics follow the applied voltage but the sensitivity of the retardation varies with time. This type of failure can corrected by changing the modulation timing.
F3	a type of failure is similar to a F2 failure but changing the modulation timing cannot correct the failure

## TECHNICAL MEMORANDUM

# DEVELOPMENT OF OPTICAL MODULATORS FOR MEASUREMENTS OF SOLAR MAGNETIC FIELDS

### Center Director's Discretionary Fund Final Report

## I. INTRODUCTION

Measurements of polarized light allow astronomers to determine the nature of the physical medium emitting or absorbing that light. In solar astronomy the scientist cannot measure the Sun's magnetic field in situ, but by using the Zeeman effect, he can relate measurements of polarized light to the magnetic field strength and direction. Since magnetic fields are related to solar activity, the measurement of polarized light is one of the most important tools to the solar astronomer. The basic component of any instrument used to analyze the polarized light emitted by the Sun is a polarization modulator. Thus, the development of stable polarization modulators with long lifetimes is important for ground-based observations of solar magnetic fields. Rotating waveplates have stable retardation properties but are slow and cannot eliminate atmospheric effects. Also quartz waveplates have a limited wavelength range and produce a spurious modulation in the transmitted beam which is related to the crystal axes. Use of electronic modulators (EM's) can eliminate these problems and EM's are used extensively in ground-based observations where their fast time response minimizes image variations due to atmospheric effects. However, all EM's that have been developed exhibit certain undesirable characteristics too, so that no single polarization modulator meets all of the requirements of the solar astronomer. Table 1 summarizes the advantages and disadvantages of four types of electronic modulators with respect to the desired design goals for solar polarimetry. Of the four, electrooptical crystals (EOC's) such as KD\*P's and liquid crystal devices (LCD's) have stable retardation characteristics and can be interfaced easily to an image system. Each has a unique property that makes them useful to the solar astronomer: the LCD operates at low voltages and has stable modulation characteristics while KD\*P modulators can be adjusted to produce any retardation and have a very high contrast ratio ( $\geq 1000$  to 1). The disadvantages are the following: KD\*P's require a high voltage ( $\approx 5500$  volts for halfwave retardance), have a limited field of view (West, 1978), and have a limited modulation lifetime. LCD modulators have a low contrast ratio and slow response times. Consequently, the goal is to systematically analyze these EM's with the aim of improving their performance.

## II. DISCUSSION

There are two areas where optical modulators are required in the MSFC Vector Magnetograph. Optical modulators are used as the polarization analyzer and as an electronic shutter to the CCD camera system (Figure 1). Each application has its own set of minimum requirements. Tables 2 and 3 summarize the requirements for the polarization analyzer and the camera shutter in the order of importance.

For the polarization analyzer the properties that are most important are those that deal with the control of the retardation properties. The contrast ratio represents the retardation resolution that can be obtained in the optics. Of equal importance is how long does it take for the retardation to stabilize and follow the modulation voltage. Even though the optical properties are important (the modulator must transmit light through it), the placement of the modulator in the collimated beam of the optics allows flaws in the modulator to be uniformly distributed over the field of view of the instrument. These optical flaws become important if they degrade the contrast ratio over the field of view of the instrument (example: strain birefringence causing variations in the optic axis over the field of view of the EM).

Although "camera shutter" is the terminology that is used to describe the application of the second electronic modulator used in the MSFC Vector Magnetograph, it is actually a light valve that synchronizes the integration time and readout time of the CCD camera system. The camera in the magnetograph is an RCA CCD with 512x320 pixel resolution. This array is divided into two areas: an integration area (320x256) and a readout area (320x256). The integration area is where the light from the Sun is converted to electrons while the the readout area, which has a mask over it, acts as an analog memory to the integration area. Figures 2a and 2b show the relationship between the polarimeter and camera shutter timing. The typical exposure time on a sunny day for the magnetograph is around 75 milliseconds, while the readout time of the CCD array is 120 milliseconds. Therefore to prevent pixel saturation, the camera shutter or light valve must control the light level so that the exposure times and the integration times match. This relaxes the requirement for a high contrast ratio (the ratio of the open and closed positions of the light valve). Although a zero light level is desirable during the time when the integration area of the CCD camera system is shifted to the readout area (Figure 2c), this property is not as important as the requirement for stable modulation properties so that errors in the optical modulator do not affect the polarimeter measurements. In order to stabilize the optical properties of a particular device, a great deal of testing and analysis has gone into the development of the timing for the magnetograph shutter; this will be discussed in greater detail in the LCD and KD\*P sections.

The following section will discuss the hardware that was developed to simulate the magnetograph timing and to test the different optical modulators.



TABLE 1. Design Goals for Electronic Modulators to be Used in the MSFC Vector Magnetograph

Design goals	Different electronic modulators			
	EOC	LCD	PEM	PLZT
Stable retardation with time	x	x		
Long lifetime		x	x	
Retardation can be adjusted	x			
Large acceptance angle		x	x	x
Adjustable timing	x	x		x
High contrast ratio	x		+	+
Low operating voltage		x	x	x
x = satisfies design goals				
+ = status unknown				

TABLE 2. Requirements for an Electrooptical Modulator Used as a Polarization Analyzer in the MSFC Vector Magnetograph

Contrast ratio greater than 1000:1
Uniform contrast ratio over 1-inch aperture
Stable modulation characteristics after 240 milliseconds
Response times less than 2 milliseconds
Optical properties(transmission, scattered light, etc.)

TABLE 3. Requirements for an Electrooptical Modulator Used as a Camera Shutter in the MSFC Vector Magnetograph

Stable modulation characteristics after 240 milliseconds
Response time less than 60 milliseconds
Optical properties
Uniform spatial response, aperture size 1-inch diameter
Contrast ratio greater than 50:1

## A. Data Acquisition System

Although the data acquisition system was developed to test either modulator under consideration, the voltage requirements and physical operation are significantly different and will be discussed in the modulator sections. The data acquisition system consisted of two computers; one to control and monitor the high voltage relays during the optical modulation tests and a second computer to act as instrument controller.

The design of the relay controller is driven by the KD\*P modulator which requires approximately 3000 volts dc to drive it to a quarterwave retardance. The LCD modulator retardance is normally determined by the physical construction of the device. The voltage applied to the LCD (between 3 and 30 volts depending on the electrode material) eliminates that retardance by mechanical rotation of the birefringent crystals. Another specification required in the KD\*P tests is the symmetric modulation of the high voltage to eliminate any dc bias which could affect the stability of the polarization measurements.

In order to test the characteristics of the optical modulators and to determine how they would perform in the MSFC Vector Magnetograph, a relay control system similar to the magnetograph (Hagyard et al., 1984) was developed. The custom relay control board is addressed by the MSC CPU through the Multibus I backplane and controls solid state relays which in turn drive the high voltage relays. To eliminate any dc biases that might occur due to drifts in a multiple power supply design used by the MSFC Vector Magnetograph, the relay control system has been designed to control the  $\pm 3000$  volt KD\*P modulation using a single power supply. Figure 3 shows a schematic of the data acquisition system. The software that was developed for the MSC CPU allows it to operate as either a standalone system (for relay testing) or as a slave to the HP9845 computer which is the data acquisition computer for the system. Communication between the two computers is through a RS232 port. Because of the requirements that the data acquisition system handle both KD\*P and LCD modulation, the relay controller had to be flexible enough to change depending on the test program. This is complicated by the fact that LCD modulators are low voltage devices (maximum voltage  $\approx 30$  dc) and KD\*P modulators require high voltages (maximum voltage  $\approx 5500$  dc for halfwave retardance). Therefore, a great deal of hardware checking is required to insure that high voltage is not applied to the inputs of the data acquisition system when the KD\*P's are being tested.

The main computer, a HP9845, controls and monitors all of the interfaces in the data acquisition system. With the exception of the RS232 interface, all of the communications between the computer and the data acquisition system is through the IEEE 488 bus.

## B. LCD Modulator

Liquid crystal devices were originally developed for low power display purposes, but because they possess the property of rotating polarized light, they are candidates for use in measurements of polarization. In the past, their time response has been poor, but recent developments have decreased their switching time between polarization states from 100 to 2 ms.

Another problem that has to be addressed before LCD's can be applied to polarization measurements is their low contrast ratio. For measurements of sources with a high degree of polarization, a low contrast ratio might not be a problem. But for measurements with weak polarizations (for example, vector magnetic fields in solar active regions), a low contrast ratio would require more image enhancements (the adding of the same polarization image) to build up a polarization map with the same signal to noise as a modulator with a high contrast ratio.

There are many types of liquid crystal compounds that could be used in the camera application. This study has been limited to compounds that have a high birefringence since they can be used in both the shutter and the polarimeter applications. Table 4 lists the LCD materials that were chosen for this study. Most of the eutectic mixtures are for use in twisted nematic cells (where the birefringence properties rotate with distance through the sample). In single compound substances the orientation of the birefringence properties depend upon the construction of the cell and whether a cholesteric material is added to the compound.

In comparing the different LCD compounds, it is convenient to describe the local alignment of a LCD sample by a unit vector  $i$ , the director, which is parallel to the long axis of the rod-like crystal. Figure 4 compares the orientation of the directors when the applied voltage is zero and  $V_{max}$  for a nematic and a twisted nematic sample. In the twisted nematic cell, the director rotates  $90^\circ$  between the two surfaces of the cell while the directors of a normal nematic cell are parallel. Normally in a uniaxial (one optic axis) nematic liquid crystal, the extraordinary index of refraction,  $n_e$ , is parallel to the director while the ordinary axis,  $n_o$ , is in the plane perpendicular to the director. Therefore, the normal nematic cell with zero applied voltage is similar in structure to a fixed waveplate with fast axis parallel (assuming  $n_e$  less than  $n_o$ ) to the director and whose retardance is dependent on the thickness of the cell. In the twisted nematic cell the fast axis rotates making it much more difficult to visualize the optical effect it has on the input polarization (Figure 5a). Basically the two components of the input polarization rotates with the principal axes of the liquid crystal while the phase difference,  $\delta$  - retardance, between them is the same as that of the untwisted nematic medium. This can be shown by integrating the difference between indices of refraction ( $n_x, n_y$ ) in the x and y direction over the thickness  $T$  of the cell. The retardation of a twisted nematic LCD is

$$\delta = \frac{2\pi}{\lambda} \int_0^T n_y(z) - n_x(z) dz$$

where  $n_y = n_o + f(z)$ ,  $n_x = n_e - f(z)$ ,  $f(z)$  = a function describing the rotation of the principal axes, and  $\lambda = 6328 \text{ \AA}$ .

Although the function  $f(z)$ , which is dependent on the birefringence of the material (Figure 5b), could be determined it is not necessary since the equation simplifies to the same relationship as the untwisted nematic sample

$$\delta = \frac{2\pi T(n_o - n_e)}{\lambda}$$

Therefore the following equation derives the thickness required to obtain a halfwave retardance for both twisted and untwisted liquid crystal compounds (Table 4):

$$T = \frac{\delta * \lambda}{(2 * \pi * \Delta n)}$$

where  $\Delta n = n_o - n_e$  = birefringence of LCD material.

TABLE 4. Thickness required for Halfwave Retardation at  $\lambda = 6328 \text{ \AA}$  for Various LCD Compounds

Material	$\Delta n$	Thickness (microns)	
		$\delta = 180^\circ(\frac{1}{2}\lambda)$	$\delta = 540^\circ(\frac{3}{2}\lambda)$
Eutectics mixtures			
E7	0.23	1.3756	4.1269
E44	0.26	1.2169	3.6507
E70	0.19	1.6652	4.9957
E80	0.16	1.9775	5.9325
Single compound			
S1115	0.12	2.6366	7.9100
S1184	0.06	5.2733	15.820
K15	0.18	1.7577	5.2733
K21	0.16	1.9775	5.9325

(Samples produced by EM Chemicals, 5 Skyline Drive, Hawthorne, NY 10532)

## 1. Camera Shutter

There are three areas that were studied to determine the feasibility of using a LCD as a camera shutter for the MSFC Vector Magnetograph: the optical response to applied voltage, the errors associated with the spatial variation of the optical properties, and the transient effects produced by the mechanical structure of the device. The transient effects will be discussed in the next section.

The digital nature of a LCD makes interfacing it to the MSFC Vector Magnetograph much easier than a KD\*P modulator. In a LCD device there is a minimum voltage ( $V_{min}$ ) that must be applied before the directors start to align to the electric field and a maximum voltage ( $V_{max}$ ) where the directors are "parallel" to the applied electric field. Increasing the voltage might improve the time response of the LCD but would not change the optical properties of the device. In the shutter application where the LCD is used as a light valve, a voltage below  $V_{min}$  is used to transmit the light to the detector and a voltage above  $V_{max}$  is used to turn the light off. The direction of the electric field is not important in this application, therefore, to improve the lifetime of the LCD by reducing any electrochemical effects due to ion migration, an alternating electric field is applied to the sample. The alternating electric field is applied to the sample by producing a phase shift in the 2 kHz squarewave voltages that are applied to each of the ITO electrodes holding the LCD material.

The second area to be considered in the application of a LCD as the shutter is the spatial variation of its optical properties. These are produced by the scattering of light in the liquid crystal material and by variations in the retardance due to thickness differences in a large aperture LCD. One technique used to control the thickness over a large aperture is to mix glass beads (diameter of beads equal to thickness required for halfwave retardation) with the liquid crystal material. Clear glass beads decrease the optical contrast of the modulator by providing a zero retardance optical path for the incident light. Light absorbing glass beads or a nonconductive grid pattern should be used to improve the polarization resolution of the device. This is especially important in the next section where a LCD is used as a variable waveplate. To minimize variations in the optical performance of the liquid crystal (and KD\*P) shutter, the shutter is mounted behind the Zeiss filter near the collimated portion of the Vector Magnetograph (Figure 1).

If the transient effect produced by the fluid motion of the liquid crystal as it responds to the applied voltage is systematic and has a repeatable time response, this effect can be neglected in the shutter application (to be discussed in more detail in the next section where this effect cannot be neglected). The only other criteria that the liquid crystal modulator must satisfy is a time response of one half of the minimum exposure time for CCD camera system (or  $\sim 35$  msec). Of the liquid crystal modulators that have been tested, the typical response time is around 5 msec.

## 2. Variable Waveplate

Normal discussions of a variable waveplate would imply that the retardation of the waveplate could be tuned either mechanically or electrically to any value needed by the optical engineer. In the shutter application, a LCD is operated below  $V_{min}$  and above  $V_{max}$  and the modulator acts as a light valve for the detector system. In the variable waveplate application, the LCD modulator must operate within that range ( $V_{min} < V < V_{max}$ ) and the retardation of the cell would be determined by the angle between the director and the applied electric field. To replace the existing KD\*P modulator in the vector magnetograph with a LCD modulator, the LCD would have to modulate between  $\pm$ quarterwave. This could be done by building a modulator whose thickness was greater than a full wave retarder and modulating the voltages between a 1/4 wave and 3/4 wave retardance. Although on paper this looks like a viable solution, the precise control of the fluid response of a liquid crystal mounted to a telescope whose environment and orientation varies with time would require a major development effort and would not properly utilize the digital nature of a LCD. If one of the quarterwave plates in the rotating waveplate assembly was replaced by a halfwave plate (see Hagyard et al., 1984, for description of the MSFC Vector Magnetograph), then a LCD modulator with a zero/halfwave modulation could be used in the MSFC Vector Magnetograph. The halfwave retardance would be set by the thickness of the cell and the polarimeter would utilize the on/off nature of an LCD. The next level of problems associated with the use of a LCD as the polarimeter arises from the boundary effects created by the sample holder. Two boundary effects that have been seen in LCD modulators are the wall effects on director orientation and a fluid motion seen in the response curve. The director orientation at the walls when an electric field is applied (Figure 4) produces a nonzero retardation and reduces the contrast ratio of the modulator. Figure 6 shows how the contrast ratio of a large aperture LCD modulator can vary both spatially and with time. By increasing the thickness of the sample to higher multiples of a halfwave retardance ( $\delta = \pi = 3\pi = 5\pi \dots$  radians), the boundary effects caused by the director orientation can be minimized but the light scattering will increase. Another technique that is being studied which would eliminate the wall errors on the director orientation is to build a match set of LCD modulators whose fast axes are separated by  $90^\circ$  and with the retardance adjusted to quarterwave plus the error in the retardance with an applied electric field. This is demonstrated by the Poincaré sphere in Figure 7.

The second boundary problem that has been seen in some of the modulators is the fluid motion of the liquid crystal material. This can be seen in the time response curve in Figure 8. To obtain accurate polarization measurements the detector would have to be synchronized to start its signal integration after the LCD retardation had stabilized. For this particular sample the signal integration would have to be delayed 100 msec which is longer than the exposure time of the camera. This delay would have a serious impact on the time resolution of the MSFC Vector Magnetograph.

### C. KD\*P Modulator

Electrooptical crystals such as KD\*P (potassium dideuterium phosphate) provide retardation proportional to the applied voltage. This property provides much more flexibility than a LCD modulator where the thickness of the cell must be adjusted to obtain a known retardance for a given wavelength. The tuning of a KD\*P to a quarterwave retardance can be done easily which makes them quite useful in eliminating cross talk between polarization measurements (West, 1985).

The electrooptical effect (which is often called the Pockel's effect) is related to the position of the deuterium atoms in the KD\*P crystalline structure (Figure 9). An asymmetry in the KD\*P structure (tetrahedron) is created when an electric field is applied producing (D-O) dipoles. This shift in the crystalline structure will then produce changes in the optical properties of the crystal (Corbridge, 1974).

Although the external field changes the energy states of the deuterium atom in the crystal, KD\*P's do not exhibit the fluid motion properties seen in LCD modulators (Figure 8). However, KD\*P modulators have their own set of problems which are related to a limited electrode lifetime and the breakdown of the crystalline structure. The KD\*P crystals that are used in the MSFC Vector Magnetograph are longitudinal modulators that are 30 mm square and 3 mm thick. A thin transparent coating (usually indium tin oxide - ITO) is placed on each side of the crystal. In some models a thin insulating material is placed between the crystal and the conductive coatings (Figure 10).

There have been three types of failures noted in our use of KD\*P modulators in the MSFC Vector Magnetograph. The first type (which will be denoted as F1) is a change in the retardation properties during a single cycle of the applied voltage (Figure 11). The second type of failure (F2) is similar to the first, in that the retardation properties change with time, but the change in the retardation properties is much slower and is related to a dc bias in the applied voltage over a long period of time. This type of failure has an additional property in which reversing the dc bias across the crystal can allow the crystal to recover its original retardation characteristics. The third type of failure (F3) is similar to a F2 failure but does not recover when the voltage is reversed. In both the F2 and F3 failures an increase in the voltage can drive the modulator to the required retardation (note voltages above 6000 volts should be avoided; at these voltages arcing through the crystal is possible and will cause irreparable damage to the crystalline structure). Although it is possible to model all of these failures by varying the characteristics of the transparent electrode, other explanations are also explored.

The F1 failures have optical responses similar to a high pass filter with a low RC time constant (Figure 11c). In these failures we have not observed a significant difference in the capacitance; therefore, we conclude that an electrical "short" exists between the two indium tin oxide electrodes. This would require a significant increase in the conductivity through the crystal ( $\approx 10^{-8}$  mho  $\text{cm}^{-1}$ ). An increase in the crystal conductivity means that the crystal structure is damaged and cannot be repaired. (Note we have assumed that the ITO electrodes have been carefully manufactured and that no obvious external short exists.)

The F3 failures have been associated with a decrease in the conductivity of the ITO electrode. This decrease in the conductivity is caused by the appearance of small islands in the electrode material where the conductive coating has disappeared (Figure 12). This failure can be corrected by recoating the KD\*P modulator.

Of all of the failure modes seen by the MSFC Vector Magnetograph, the F2 is the most serious because the retardation of the KD\*P is changing slowly and is difficult to monitor in real time. Although a change in the retardation with a fixed dc voltage has been mentioned in the literature (Bennett and Bennett, 1978), no physical explanation of this property was given. In 1966 Kaminow and Turner noted that, although a KD\*P crystal can be grown relatively strain free, a modulating field can strain a crystal by producing thermal gradients. When the electric field is removed, the thermal gradients disappear and the crystal returns to its original state. The F2 failure is different from the problem observed by Kaminow since it appears to have memory and will not recover unless a reverse bias is applied to the crystal. For example, if a polarization measurement requires the square wave cycling of the KD\*P between 0 and 1/2 wave retardation and a F2 failure occurs, turning the KD\*P off will not correct the failure. But reversing the electric field by modulating between 0 and -1/2 wave would cause the KD\*P to recover. Therefore the F2 failure is related to ion migration in the KD\*P modulator which affects the electrical properties of the ITO coating.

ITO coatings are in an amorphous state when they are first sputtered onto the substrate (glass or KD\*P) and are susceptible to further oxidation. Oxygen vacancies make up a major contribution to the electron carrier concentration in the ITO coating, and controlling the oxidation rate is critical in determining the conductivity of the sample. If the coatings are baked in an oven at 500 °C, the strain and crystal imperfections in the ITO coating can be removed minimizing any further oxidation of the coating (which would decrease the conductivity). KD\*P's undergo a phase change at 100 °C. If the ITO coating is placed on the KD\*P substrate, the modulator must be placed in a sealed housing or in an oxygen-deficient environment immediately after the coating is completed. This leaves the ITO coating in the amorphous state, and any future exposure to oxygen (or other elements that could fill the oxygen vacancies) can change its electrical characteristics. The contamination source for the ITO coatings is either the KD\*P crystals or the silicon cement that is used to protect the coatings (and the KD\*P which is hygroscopic) from the environment.

The resistivity through KD\*P crystals is very high (Table 5) and has been difficult to monitor for real time changes. Also measurements before and after a failure have shown no changes in the capacitance of the KD\*P modulator. This could be due to the fact that the measured capacitance is related to the thickness of the KD\*P crystal under the gold electrodes (see Figures 10 and 13) and that the measurements are not sensitive to any crystalline changes under the ITO coatings. The placement of metal probes at various locations on the KD\*P surface may be required in future measurements to determine if localized failures in the crystalline structure can account for the ion migration or if the ion migration is uniform across the crystal.



TABLE 5. Resistivity of KD\*P samples. (Values in the table are divided by  $10^{10}$  ohm  $\text{cm}^{-1}$ .)

Crystal No.	Deuteration Level		
	90% $\rho$	95% $\rho$	99% $\rho$
1	7.7	2.1	2.3
2	7.8	2.3	2.3
3	7.4	2.2	2.2
4	13.0	2.0	2.3
5	19.0	2.2	2.5
6	9.8		
7	9.9		
8	26.0		
9	16.7		
10	10.5		
11	11.0		

See Appendix A for discussion on how the resistivity was measured.

To reduce the ion migration through the KD\*P to the ITO coating interface, an insulating material (silicon monoxide) was placed between them (Figure 13b). The oxidation rate of this coating is also very important. Excessive oxidation ( $\text{SiO}_2$ ) produces coatings that have poor mechanical stability and allows the material to flake off of the crystal. Too little oxidation will produce a "leaky" capacitor that is very temperature sensitive (Berry et al., 1968).

To simplify the coating process the ITO coating can be applied to two glass windows and the KD\*P mounted between them. An air gap between the KD\*P and the windows might minimize ion migration but arcing (which can occur at voltages as low as 400 volts) between the electrode and the KD\*P can damage the crystal. To eliminate the arcing an insulating optical grease is placed between the ITO coating and the KD\*P crystal. Unfortunately the optical grease, which is used to eliminate the arcing, can also be a source of contamination. Electrolysis between the optical grease and the ITO coating will produce a chemical reaction and a discoloration of the KD\*P electrode. Although recovery of the modulation characteristics is possible by reversing the electric field, continued use of a bias field will create a F3 failure.

Another solution that has not been studied is the application of a thin metal coating that does not use oxygen vacancies to produce a conductive coating. These coatings have two problems associated with them: thickness (conductivity) versus transmission loss and poor mechanical strength in thin coatings.

Finally, a voltage modulation scheme has been developed to stabilize the retardation properties of existing KD\*P modulators in the MSFC Vector Magnetograph.

These schemes will be discussed in greater detail in the next two sections. The modulation schemes are based on the following assumptions: that the frequency of the applied voltages must be much faster than the time for ion migration through the crystal (F1 failure) and that there is no integrated dc bias in the voltage across the crystal to produce ionic migration (F2 failure).

## 1. Variable Waveplate

The reason for the development of a new polarimeter for the MSFC Vector Magnetograph in 1983 was to eliminate the F2 failures (Hagyard et al., 1984). Although it represented a significant improvement over the original two KD\*P polarimeter, small retardation errors in the quarterwave plates, birefringence in the fore optics of the telescope, and strain induced birefringence in the KD\*P (West, 1985) required a dc bias in the voltage modulation to correct for those errors. Although the dc bias was small ( $\approx 200$  volts) compared to the that of the original polarimeter (4000 volts), the F2 failure could still be seen in some of the KD\*P modulators. Although realtime monitoring and correction of the polarimetry data was important in the original polarimeter (where the turnaround time between acquired data and analyzed data averaged 2 weeks), the "real" time analysis ( $\approx 30$  minutes) of the new Magnetograph can monitor the status of the polarimeter. In the new Magnetograph it is more important to increase the stability of the polarimeter by providing symmetric dc modulation (Figure 2a) and correct for hardware errors in the software. Hardware correction of hardware errors (retardation) can only work when they do not induce new errors (F2 failures). Therefore, until an electrode can be developed that will produce stable retardation properties, KD\*P modulators should be used with symmetric dc modulation.

## 2. Camera Shutter

The use of an electrooptic modulator as a shutter requires a  $180^\circ$  phase shift (halfwave retardance) in the electric vector between the on and off state. The design of the original KD\*P shutter included a quarterwave plate (quarterwave =  $90^\circ$  phase shift) so that the maximum voltages across the KD\*P would be  $\pm$  quarterwave ( $\approx 2000$  volts). With the fast axes of the quarterwave plate and the KD\*P aligned, the apparent phase shift of the shutter was  $0^\circ$  and  $180^\circ$ . The problem with this type of modulation scheme is shown in Figure 2e. The average electric field across the KD\*P shutter depends on the exposure and readout time of the CCD camera. Unless the exposure time is exactly one half of the readout, there will be a dc bias in the applied voltage. Therefore to guarantee that

$$\int_0^{t_1} V(t)dt = 0$$

the quarterwave plate was eliminated from the shutter and the KD\*P was cycled between  $\pm$  halfwave (Figure 2f). Although this should guarantee a stable response in the KD\*P shutter any small errors in the applied voltages caused by voltage

drops in the high voltage relays, variations in the high voltage power supplies, or strains in the crystal that require dc biases to obtain  $\pm \frac{\lambda}{2}$  retardances would create a bias in the polarimetry measurement (Figure 2a). Therefore, to guarantee that any errors in the shutter would average to zero and would not affect the polarization measurement, an odd modulation scheme was developed (Figure 2g) where the halfwave voltages were applied in following periodic fashion:

$$V_o = [(+, -, -, +, +, -, -, +), (-, +, +, -, -, +, +, -), (+, -, -, +, +, -, -, +), \dots]$$

Defining a group of positive and negative halfwave pulses to be:

$$I = -J = [+ , - , - , + , + , - , - , +]$$

where the (+, -) signs represent positive and negative halfwave pulses ( $\pm 2000$  volts dc) with the same time duration. The shutter modulation is then a set of (I,J) pulses:

$$V_o = [I, J, I, J, I, \dots]$$

The completion of an (I,J) cycle will produce the same number of  $\pm$  halfwave pulses in the positive (defined as an A cycle) and negative (B cycle) quarterwave cycles of the polarimeter but in a modulation scheme were the difference in the A/B measurements should represent the measured polarization and not some small error in the camera shutter.

### III. CONCLUSIONS

The goal of this project was to develop and test optical modulators that could be used in the MSFC Vector Magnetograph. The data acquisition system that was developed provides software control of the modulation timing and allows the scientist to study the response and lifetime of KD\*P and LCD modulators. Using this system the spatial and temporal response of several LCD modulators have been tested to see how they would affect magnetograms if they were used as the optical shutter in the MSFC Vector Magnetograph. Although their optical contrast has been a problem with the samples tested to date, their effect on the integrated difference (A-B difference) is minimal and LCD modulators could be used in the MSFC Vector Magnetograph to control the readout rates of the CCD camera system.

Although the CDDF development program ended September 30, 1986, testing of LCD and KD\*P modulators will continue under the ground-based RTOP 188-38-52. This additional testing is needed to provide better statistics on how voltage timing, electrode structure, and chemical composition affect modulator lifetime.

## REFERENCES

- Bennett, Jean M and Harold E. Bennett, 1978, in Handbook of Optics, ed. Walter G. Driscoll, McGraw-Hill Book Company, 10-141.
- Berry, Robert W., Peter M. Hall and Murray T. Harris, 1968, Thin Film Technology, D. Van Nostrand Company, Inc., 379.
- Corbridge, D. E. C., 1974, The Structural Chemistry of Phosporus, Elsevier Scientific Publishing Company.
- Hagyard, M. J., E. A. West and N. P. Cumings, 1984, "The New MSFC Vector Magnetograph," NASA TM-82568.
- Kaminow, I. P. and E. H. Turner, 1966, Applied Optics , 5, 1612.
- West, Edward A., 1978, Applied Optics, 17, 3010.
- West, E. A., 1985, Measurements of Solar Vector Magnetic Fields, NASA Conference Publication 2374, 160.

## APPENDIX: Resistivity Test

The resistance of each crystal was measured by placing each crystal in a dry nitrogen purge box. The 30 x 30 mm surfaces of the KD\*P samples were painted with Acheson Aqua-Dag to provide the conducting electrodes. A Keithly electrometer was then used to measure the resistivity of the samples. The resistivity was calculated from the following formula.

$$\rho = R \frac{A}{T}$$

where  $\rho$  = resistivity,  $R$  = measured resistance through crystal,  $A$  = area of electrodes, and  $T$  = thickness of crystal.

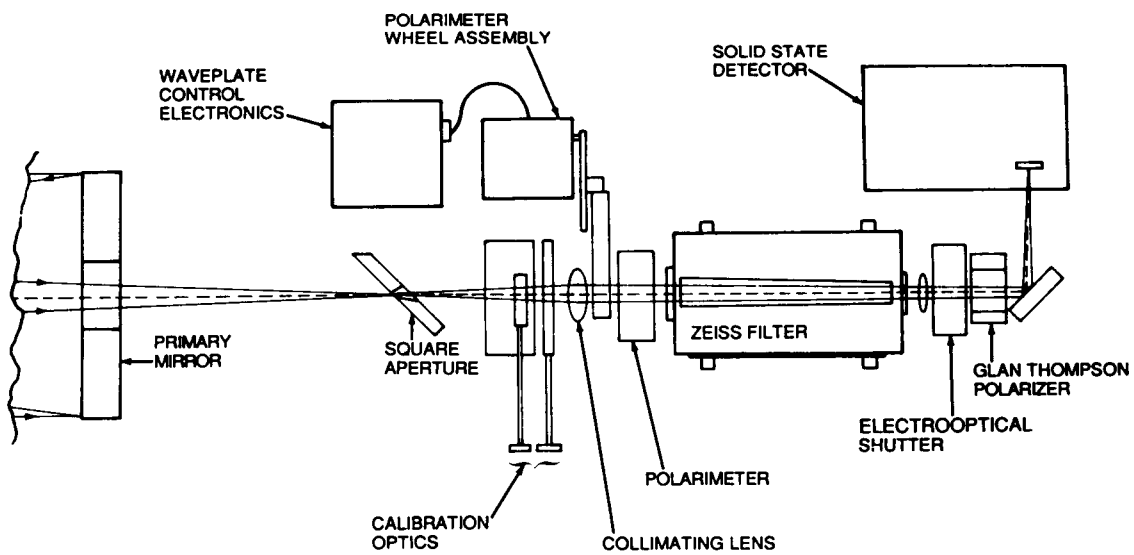


Figure 1. Schematic diagram showing the location of the shutter and polarimeter electrooptical modulators used in the Marshall Space Flight Center Vector Magnetograph.

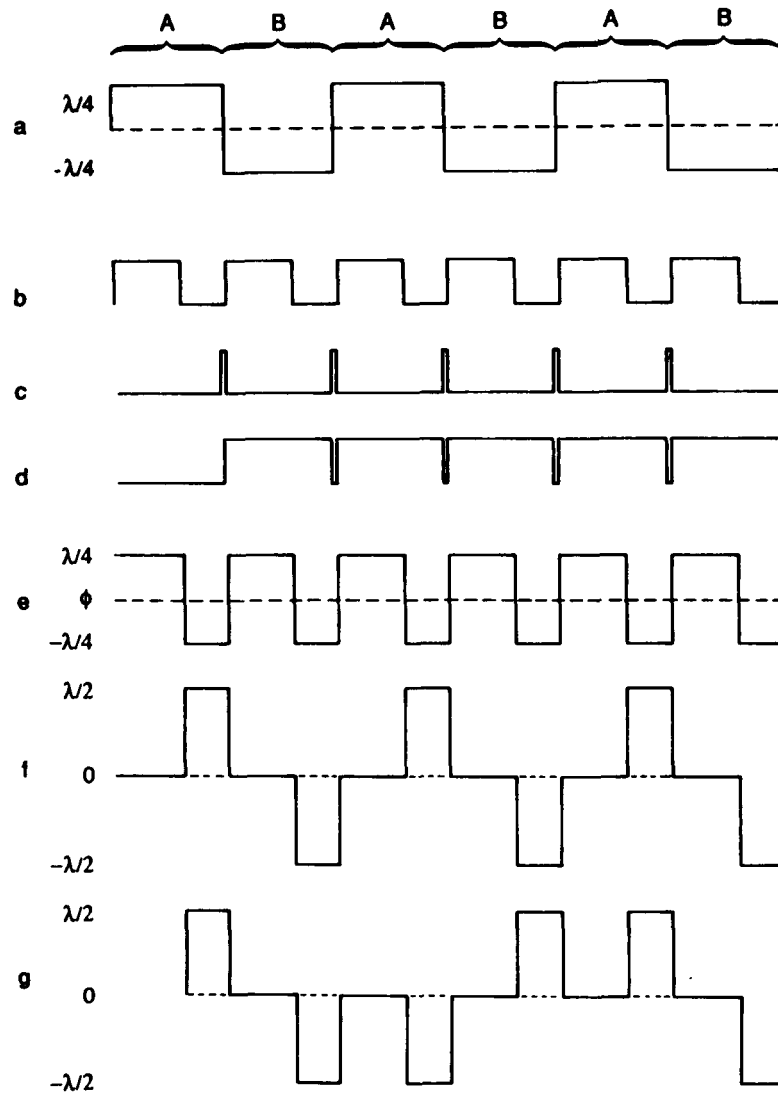


Figure 2. Timing diagram showing the relationship between the polarimeter timing and the shutter timing required for LCD and KD\*P modulators. Curve (a) defines the  $\pm$  quarterwave modulation of the polarimeter, the A cycle is defined by the  $+\frac{\lambda}{4}$  retardation, the B cycle is the  $-\frac{\lambda}{4}$  retardation. Curve (b) is the camera exposure, curve (c) the camera shift, and curve (d) the camera readout timing. Curves (e,f,g) define different modulation schemes used in the camera shutter application

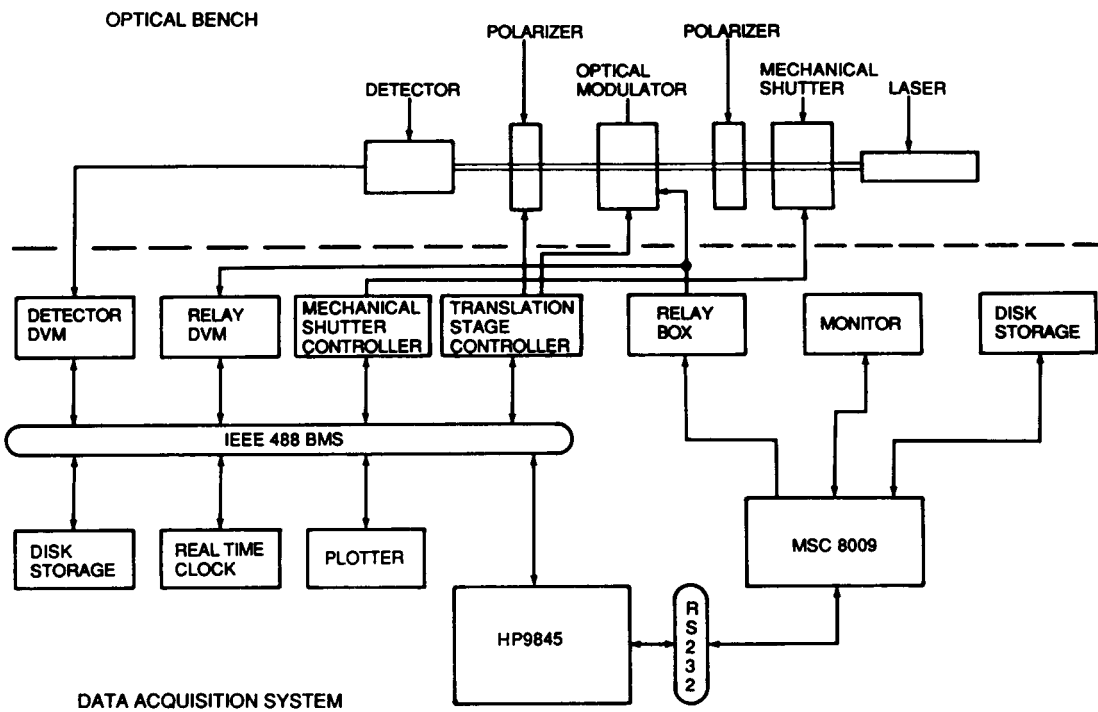


Figure 3. Diagram showing the optical components used in polarization tests and the data acquisition system



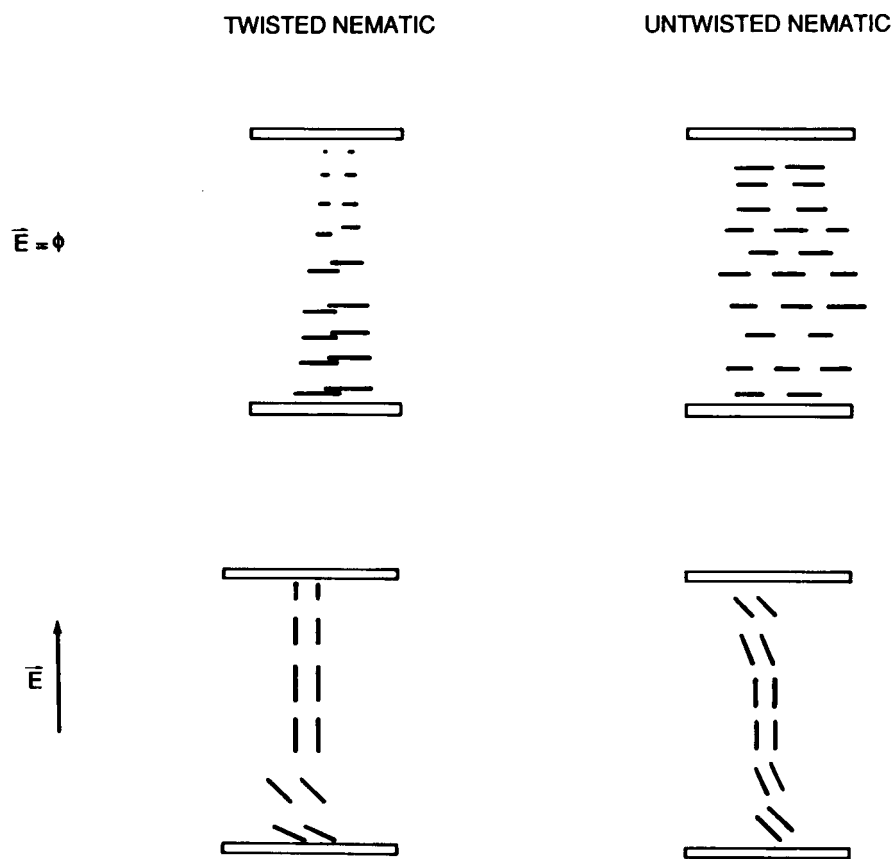
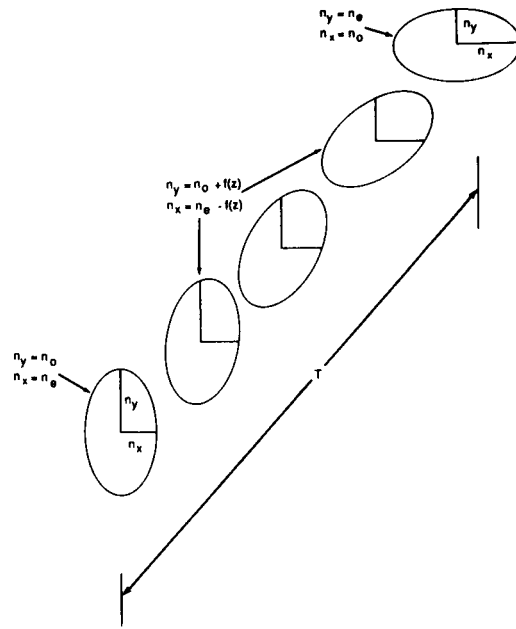
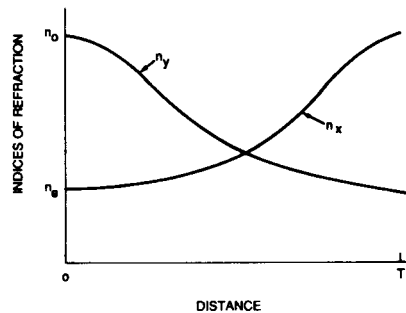


Figure 4. Diagram of the director orientation for an untwisted and twisted nematic liquid crystal in the presence of an electric field



a.



b.

Figure 5. The orientation of the indices of refraction in a twisted nematic LCD. The top diagram (a) shows how the ellipse that describes in birefringence properties of the twisted LCD rotates with distance through the sample. The lower diagram (b) describes the change in the indices of refraction using a fixed coordinate system.

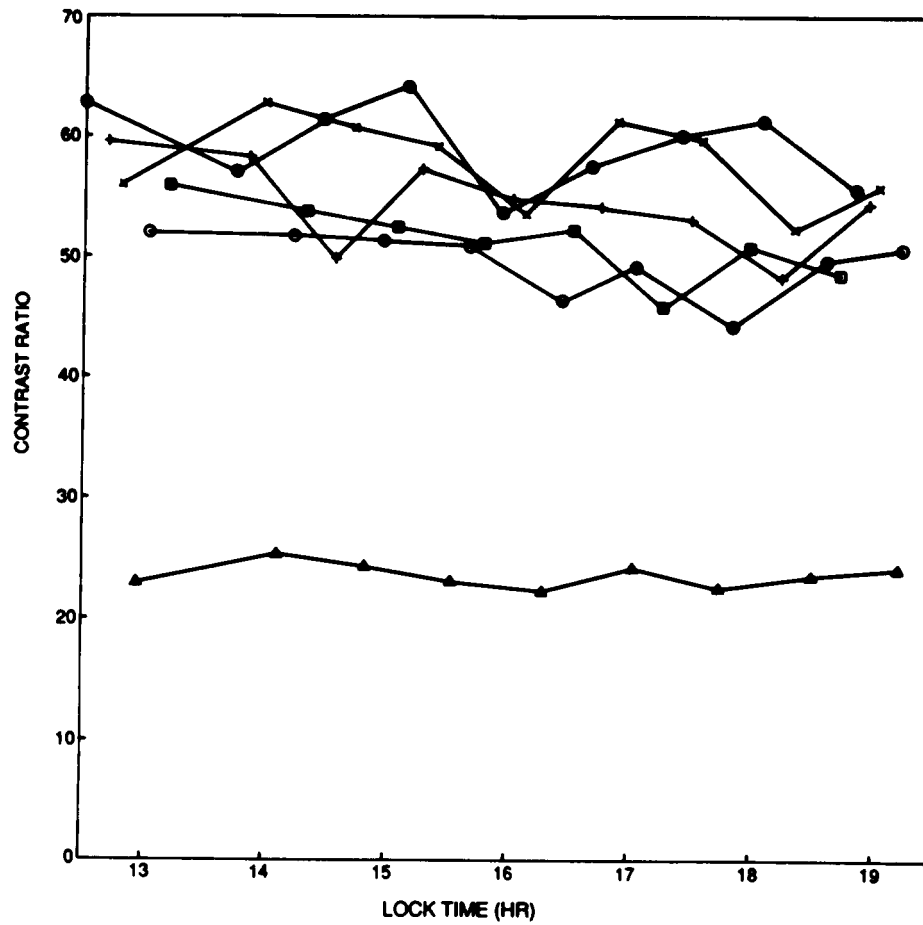
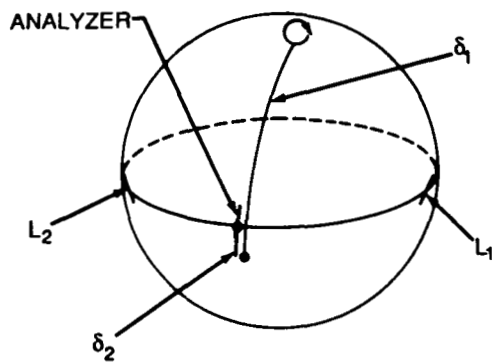


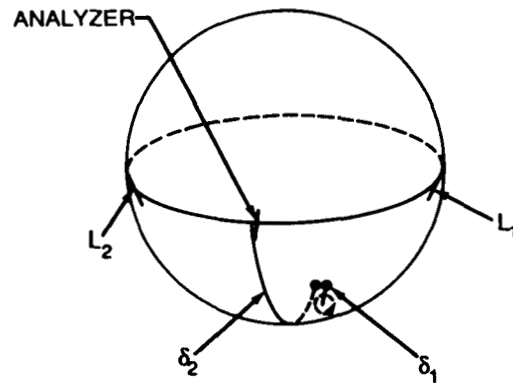
Figure 6. Curves showing the spatial and temporal variation in the contrast ratio of a liquid crystal modulator. The bottom curve has a very low contrast ratio which was due to a transparent spacer that was in the optical path. This spacer controls the sample thickness/retardation for the LCD modulator.



$$V_1 = \phi, V_2 = V_{\max}$$

$$\delta_1 = 90^\circ + \delta_\epsilon, \delta_2 = \delta_\epsilon$$

a



$$V_1 = V_{\max}, V_2 = \phi$$

$$\delta_1 = \delta_\epsilon, \delta_2 = 90^\circ + \delta_\epsilon$$

b

Figure 7. Poincaré sphere showing the fast axis orientation ( $L_1, L_2$ ) and retardation ( $\delta_1, \delta_2$ ) of two LCD modulators aligned to reduce the retardation errors ( $\delta_\epsilon$ ) caused by the boundary effects on the director orientation. The  $+\frac{\lambda}{4}$  retardance (a) is produced by the the first LCD ( $V_1 = 0$ ) whose thickness is set to  $\frac{\lambda}{4}$  plus the retardation error ( $\delta_2 = \delta_\epsilon$ ) of the second LCD. The  $-\frac{\lambda}{4}$  retardance (b) is produced in a similar way. The orientation of the fast axis ( $L_1, L_2$ ) determines the sign of the retarder.

ORIGINAL PAGE IS  
OF POOR QUALITY

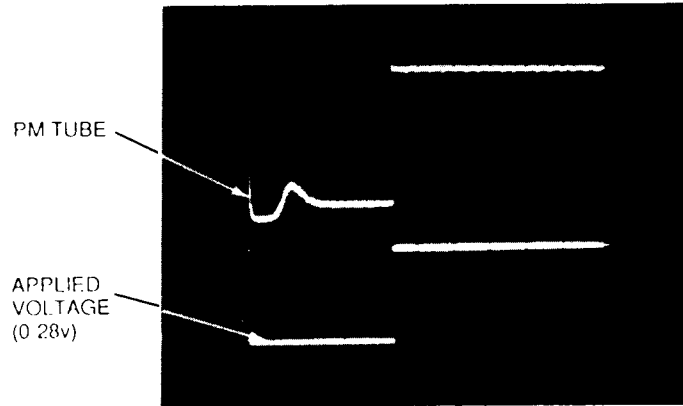


Figure 8. The time response of a large LCD modulator. Each division is 50 msec.

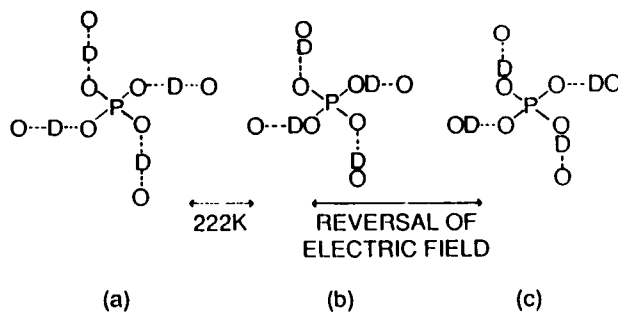


Figure 9. Diagram showing the movement of the deuterium atom in the KD\*P crystal with an applied electric field

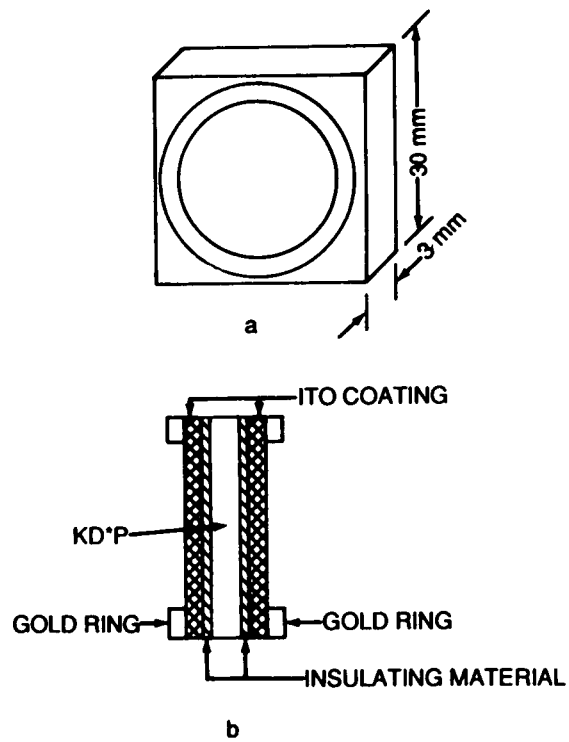
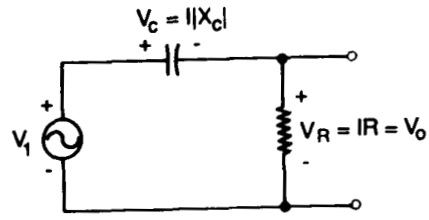
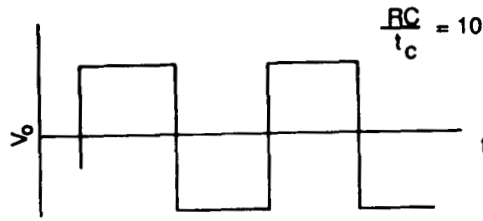


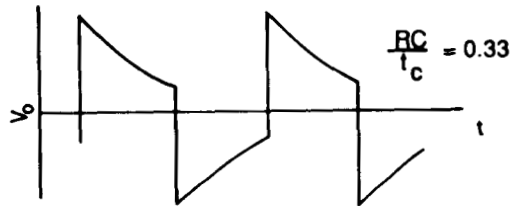
Figure 10. Schematic of a KD\*P modulator with the electrode and insulating coatings



a



b

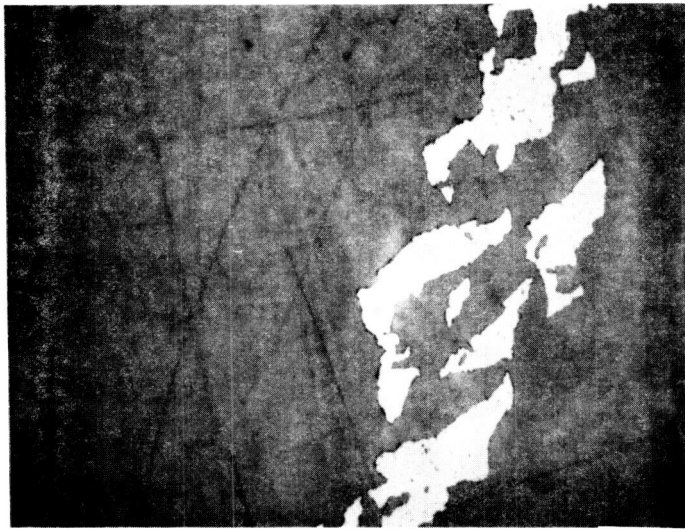


c

Figure 11. Diagram of the electrical equivalent for a KD\*P modulator (a). The optical response ( $V_o$ ) should follow the square wave modulation of the input source ( $V_1$ ) in an ideal KD\*P modulator (b). The response of a KD\*P modulator having a low RC time constant (c).



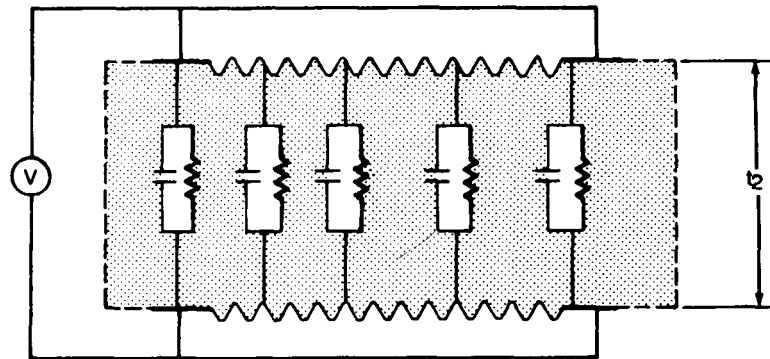
a



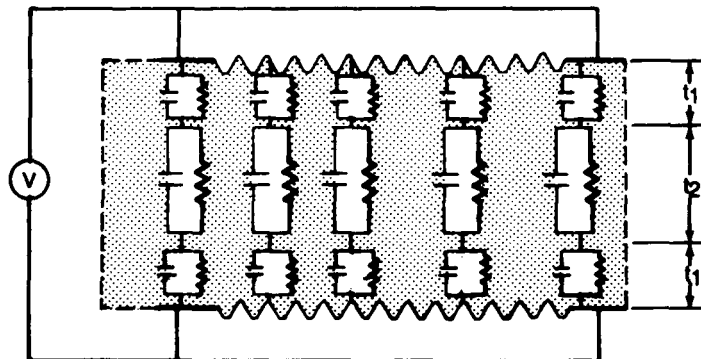
b

Figure 12. Pictures showing areas of high resistivity where the ITO coating has disappeared. The upper picture shows the interface between the 1 -inch gold ring and the ITO coating. The lower picture (b) shows a typical area  $\frac{1}{8}$  inch inside the gold electrode.





a KD\*P ONLY



b KD\*P WITH SILICON MONOXIDE INSULATOR

Figure 13. Schematic showing that the resistivity and capacitance across a KD\*P modulator varies with the crystal properties, uniformity of the ITO coating (a), and the electrical properties of the insulating material (b).

APPROVAL

DEVELOPMENT OF OPTICAL MODULATORS FOR MEASUREMENTS  
OF SOLAR MAGNETIC FIELDS - CENTER DIRECTOR'S  
DISCRETIONARY FUND FINAL REPORT

By E. A. West and J. E. Smith

The information in this report has been reviewed for technical content. Review of any information concerning Department of Defense or nuclear energy activities or programs has been made by the MSFC Security Classification Officer. This report, in its entirety, has been determined to be unclassified.

*E. Tandberg-Hanssen*

---

E. TANDBERG-HANSSSEN

Director, Space Science Laboratory

1. REPORT NO. NASA TM- 100315		2. GOVERNMENT ACCESSION NO.		3. RECIPIENT'S CATALOG NO.	
4. TITLE AND SUBTITLE Development of Optical Modulators for Measurements of Solar Magnetic Fields - Center Director's Discretionary Fund Final Report				5. REPORT DATE October 1987	
				6. PERFORMING ORGANIZATION CODE ES52	
7. AUTHOR(S) E. A. West and J. E. Smith				8. PERFORMING ORGANIZATION REPORT #	
9. PERFORMING ORGANIZATION NAME AND ADDRESS George C. Marshall Space Flight Center Marshall Space Flight Center, Alabama 35812				10. WORK UNIT NO.	
				11. CONTRACT OR GRANT NO.	
				13. TYPE OF REPORT & PERIOD COVERED Technical Memorandum	
12. SPONSORING AGENCY NAME AND ADDRESS National Aeronautics and Space Administration Washington, D.C. 20546				14. SPONSORING AGENCY CODE	
15. SUPPLEMENTARY NOTES Prepared by Space Science Laboratory, Science and Engineering Directorate.					
16. ABSTRACT  The measurement of polarized light allows solar astronomers to infer what the magnetic field is on the Sun. The accuracy of those measurements is dependent on the stable retardation characteristics of the polarization modulators used to minimize the atmospheric effects that are seen in ground-based observations. This report describes the work by the Space Science Laboratory at Marshall Space Flight Center as part of the Center Director's Discretionary Fund to improve two types of polarization modulators. As a result of this program, the timing characteristics for both electrooptic crystals (KD*Ps) and liquid crystal devices (LCDs) have been studied and will be used to enhance the capabilities of the MSFC Vector Magnetograph.					
17. KEY WORDS  Polarization, Polarization Modulators, Electrooptics, Polarized Light			18. DISTRIBUTION STATEMENT  Unclassified--Unlimited  <i>E. A. West</i>		
19. SECURITY CLASSIF. (of this report)  Unclassified		20. SECURITY CLASSIF. (of this page)  Unclassified		21. NO. OF PAGES  34	22. PRICE  NTIS